PAPER 4

Geothermics 72 (2018) 101–111

Contents lists available at ScienceDirect

Geothermics

journal homepage: www.elsevier.com/locate/geothermics

Thermal conductivity characterization of three geological formations by the implementation of geophysical methods

Cristina Sáez Blázquez*, Arturo Farfán Martín, Pedro Carrasco García, Diego González-Aguilera

Department of Cartographic and Land Engineering, University of Salamanca, Higher Polytechnic School of Avila, Hornos Caleros 50, 05003 Avila, Spain

ARTICLE INFO

Keywords:
Low enthalpy geothermal installations
Thermal conductivity
Multichannel analysis of surface waves
Seismic refraction
Wave's velocities

ABSTRACT

In very low enthalpy geothermal installations it is essential to know the thermal conductivity parameter of the surrounding ground. The present study uses seismic prospecting as a basis for the knowledge of the mentioned thermal property. Using the technique of Multichannel Analysis of Surface Waves (*MASW*) and seismic refraction, it has been possible to correlate the velocity of the *P* and *S* waves with the thermal conductivity of three study areas. Continuous measurements of the thermal conductivity parameter were performed on samples from the areas where the seismic prospecting was made. The maximum and minimum thermal conductivity values were connected to the highest and lowest *P* and *S* wave's velocities. From this relation, an interpolation between the couple of values allows to obtain a linear equation used to predict the intermediate thermal conductivity values. As a result, graphs of thermal conductivity against *P* and *S* wave's velocities were created for each of the study areas. Additionally, 2D images of the spatial distribution of the thermal conductivity of the subsoil of each formation were performed. Thus, seismic prospecting allows, besides knowing the geology of the subsoil, the possibility of estimating the thermal conductivity of a certain ground. This parameter is indispensable for the subsequent process of calculation and dimensioning of a very low temperature borehole heat exchanger.

1. Introduction

The growing demand of very low enthalpy geothermal installations encourages paying special attention in the design of these systems. An incorrect dimensioning could cause important consequences in the short and long term operation. It is therefore fundamental to carry out an exhaustive analysis of the ground where the installation will be placed.

In this context, the thermal conductivity of the surrounding ground is especially important. This parameter influences the thermal exchange between the ground and the rest of components of the installation. Thus, the value of this property affects the drilling length required to cover some specific needs (Blázquez et al., 2016). The thermal conductivity is an important physical property for predicting heat flow and corresponding subsurface temperatures (Haenel et al., 1988; Rühaak et al., 2015; Rühaak, 2015). It describes how well the heat is conducted through a material.

Although it is still difficult to estimate the thermal conductivities of rocks at a large scale required for geothermal applications, different methods currently estimate it for full geological formations, sections or boreholes (Fuchs and Balling, 2016a; Fuchs and Balling, 2016b). In this context, tools as the optical scanning technique, allows providing measurements on cores samples directly (Popov et al., 2016). At present, there is tabulated information that assigns a value of thermal conductivity to each geological formation. It associates an approximate thermal conductivity value to a certain material without cost. However, its precision is quite low given that the thermal conductivity can still vary considerably, even for the same rock type (Cermak and Rybach, 1982). The opposite case would be the execution of a Thermal Response Test (*TRT*) in the corresponding ground. It provides an accurate thermal conductivity value despite the additional cost that this test involves. There are also numerous devices that measure the thermal conductivity of a material from samples analyzed in the laboratory. The controversy of these methods is that the whole rocky formation is not considered and the thermal conductivity results do not represent all the ground (Blázquez et al., 2017; Barry-Macaulay et al., 2013; Liou and Tien, 2016; Kukkonen and Lindberg, 1995; Lira-Cortés et al., 2008; Jorand et al., 2013; Krishnaiah et al., 2004).

For these reasons, it is important to look for alternatives to estimate the thermal conductivity of the whole geological formation that surrounds the borehole heat exchanger. The implementation of these techniques should not constitute an impediment from the economic point of view.

The integration of secondary data, like seismic velocities

* Corresponding author.
E-mail address: u107596@usal.es (C. Sácz Blázquez).

https://doi.org/10.1016/j.geothermics.2017.11.003
Received 21 June 2017; Received in revised form 2 November 2017; Accepted 2 November 2017

measurements could constitute an excellent option to balance the accuracy and the representation of the thermal conductivity results with the cost that its execution entails (Esteban et al., 2015; Pimienta et al., 2014). Before drilling the geothermal borehole/s, it is necessary to know the subsoil materials to choose the most suitable drilling method. Generally, seismic prospecting is commonly used for such purposes. The present research suggests the use of this technique with an additional aim: estimating the thermal conductivity parameter of the ground where is used. Thus, seismic prospecting would allow knowing the geological composition of a certain ground and in turn, its thermal conductivity by the correlation of this property with different seismic parameters.

The occurrence of a similar trend between thermal conductivity and compressional wave velocity has sufficiently been demonstrated in numerous previous studies (Balling et al., 1981; Fuchs et al., 2015; Gegenhuber and Schoen, 2012; Hartmann et al., 2008; Özkahraman et al., 2004a; Özkahraman et al., 2004b; Popov et al., 2003). This is why the principal objective of this research is to combine thermal conductivities from laboratory measurements and seismic velocities from in situ seismic prospecting. Thermal conductivity measurements are carried out on samples analyzed in the laboratory (rocks) or directly in their original place (loose materials). Seismic profiles are made throughout the study area where samples are collected to measure the thermal conductivity parameter. The principal purpose of this study is correlating both parameters: by the use of real seismic and thermal conductivity measurements and without model predictions. Thus, results will be completely representative of the area in question given the basis on real data. The final results provide a 2D thermal conductivity image of each area where the present methodology was implemented.

2. Materials and method

2.1. Theoretical basis

Geophysics includes a large number of techniques whose aim is the study of the Earth's crust materials. Throughout this work these techniques and the resulting parameters from them were analyzed to find a logical relation between them and the thermal conductivity. After an exhaustive analysis and study of state of the art, the seismic prospecting methods were selected as potential candidates to achieve the objective of this work.

Seismic prospecting techniques are based on the measurement of the arrival times of the *P* and *S* waves generated on the ground by a particular mechanical energy source. These waves are transmitted from a point to another where sensors (geophones) are connected to a seismograph recorder.

The way in which the seismic waves are transmitted through the ground presents a great similarity to the way in which the heat is transmitted by the mechanism of conduction. The propagation velocity of seismic waves in the ground is different depending on each material, as in the case of the heat conduction. In most cases, both parameters have a directly proportional relation ([Özkahraman et al., 2004a,Özkahraman et al., 2004b]Özkahraman et al., 2004a; Özkahraman et al., 2004b), although, for certain materials and conditions this positive trend is not always observed (Fuchs and Förster, 2014; Gegenhuber, 2011). In this research, the positive correlation between both parameters was previously verified by in situ measurements in the study areas subsequently defined.

Thus, for the same geological composition, the transmission velocity of the seismic waves is higher in hard and compact rocks and lower in the case of poorly consolidated rocks. In the same way, the thermal conductivity of a ground is higher if the compaction and consolidation of that material is also high.

For a given material, its state of maximum deterioration and decomposition corresponds to the minimum velocity at which *P* and *S* waves propagate through it. In contrast, the state of maximum consolidation and compaction of a formation corresponds to the highest velocity at which these waves are capable of being transmitted through it. Also, the thermal conductivity for that material will have the lowest value for its state of maximum decomposition and its highest value for its state of maximum consolidation.

Based on this fact, (and given the directly proportional relation between *P* and *S* waves' velocity and thermal conductivity) it is possible to establish a correlation between the propagation velocity of these waves in a given material and its thermal conductivity.

By carrying out seismic prospecting on a particular area and on the basis of its geology, some relevant information can be deduced:

- Distribution of materials in the subsoil.
- Detection of the most altered areas (maximum state of alteration) and those ones that present the maximum state of compaction. Each of these areas has an assigned velocity value of the *P* and *S* waves.

By taking samples of these zones and measuring the thermal conductivity of each one, we obtain the initial and final points of a relation between the seismic velocities and the thermal conductivity. From this pattern, it is possible to know by thermal seismic tests the thermal conductivity at any place (constituted by any of the materials tested in this article) where the geothermal installation will be placed.

Table 1
Study areas selected in the present research.

Area	Location	Rock type
1	40°37'37.57"N 4°36'38.45"O	Schists
2	40°39'48.99"N 4°42'47.27"O	Medium grain adamellite
3	40°39'23.68"N 4°40'13.99"O	Coarse-grained adamellite

2.2. Materials (Techniques)

Seismic prospecting and thermal conductivities used in this work were the following:

2.2.1. Seismic measurements

The exploration techniques used to achieve the objective of the present research are included in the seismic field:

2.2.1.1. Multichannel analysis of surface waves (MASW). It is a non-destructive seismic method that evaluates the thickness of the pavement as well as the linear elastic modules of the materials placed under this pavement (Park et al., 1999). This method analyzes the dispersion properties of the surface seismic waves, which horizontally propagate along the surface from the impact point to the receivers.

A set of receivers distributed along short (1–2 m) and long (50–100 m) distances simultaneously record the emissions from an impulsive or vibratory source. Statistical redundancy is provided to measure phase velocities. Multichannel data show a variable frequency format over time. From the analysis of these data it is possible the identification and rejection of non-fundamental Rayleigh waveforms and incoherent noise (Louie, 2001).

In the present work, MASW tests were carried out using a device of 10 (area 1) and 12 (area 2 and 3) geophones of 4.5 Hz placed every 5 m. The working methodology involved the execution of a series of shots by a 20 kg tenderiser. The equipment used in these tests was the commercially known as "Stratavisor Nx" belonging to "Geometrics". This device has 60 channels and an auto-calibration option.

After the execution of the in situ MASW tests, data were extracted and processed by the "Surface Wave Analysis Wizard" module of the software "Seisimager". This software allows obtaining the *S* wave by

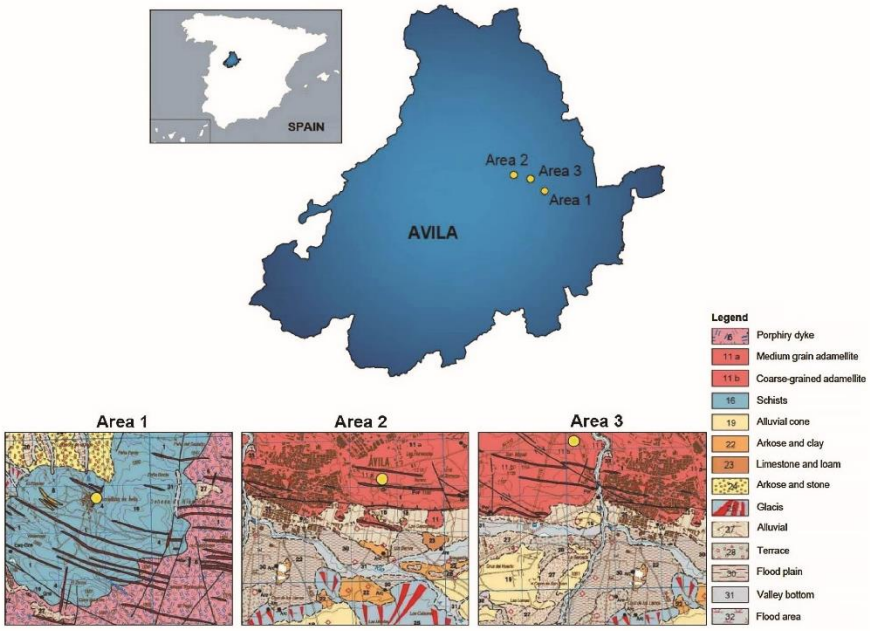

Fig. 1. Geological characterization of the three study areas.

the analysis of the frequencies and phase velocities of the surface seismic waves. Additionally, a series of secondary data (presented in Section 3. Results) are automatically calculated and provided by this equipment.

2.2.1.2. Seismic refraction. The other prospecting technique used in this study is based on seismic refraction. It consists of the generation of seismic waves by a hammer or an explosive, and the recording of those waves that suffer total refraction along the contacts of variable velocity layers. In this case, the recorded waves are the primary or longitudinal *P* waves, in which particles move in the propagation direction of the wave, by compressions and dilations.

This system records the arrival times of waves produced by impacts of a hammer on a steel sheet placed in the surface of the ground until its arrival to a set of geophones. These devices transform the ground vibrations produced by the waves into electrical signals.

Seismic refraction uses the times of the first arrivals in the seismograph. These arrival times correspond to the refracted waves in the different subsoil layers. Each of these layers is distinguished by its acoustic impedance called refractor.

As a result of the application of this method, a ground seismic image was obtained in the form of a velocity section (V (x,z)).

Each seismic refraction profile was 50 m in length (area 1) and 60 m in length (area 2 and 3) with geophones placed every 5 m, shooting at the ends and center of each profile.

2.2.2. Thermal conductivity measurements

Measurements of the thermal conductivity parameter were carried out using the KD2 Pro equipment developed by Decagon Devices (Decagon Devices, 2016). This device is constituted by a portable controller and a sensor (RK-1) that makes possible the measurement of the thermal conductivity of rocks or previously compacted soils.

Its operation is based on the infinite line heat source theory and computes the thermal conductivity by monitoring the dissipation of heat from the needle probe. Heat is applied to the needle for a set heating time *th*, and temperature is measured in the monitoring needle during heating and for an additional time equal to *th* after heating. The temperature during heating is deduced from Eq. (1).

$$T = m_0 + m_2 t + m_3 ln t \tag{1}$$

Where:

m_0 is the ambient temperature during heating

m_2 is the rate of background temperature drift

m_3 is the slope of a line relating temperature rise to logarithm of temperature

Eq. (2) represents the model during cooling.

$$T = m_1 + m_2 t + m_3 ln \frac{t}{t - t_h} \tag{2}$$

Both Eqs. (1) and (2) are used by the equipment to provide the temperatures during the period of heating and after it when heating stopes and needle starts cooling.

Thermal conductivity is calculated from Eq. (3) that also considers the heat flux *(q)*.

$$k = \frac{q}{4m_3} \tag{3}$$

Only 2/3 of the data collected are used during heating and cooling (it ignores early-time data) since these equations are long-time approximations to the exponential integral equations. It helps to prevent errors derived from the placement of the needle. Eqs. (1) and (2) can be solved by linear least squares, giving a solid and more adjusted result (Kluitenberg et al., 1993; Shiozawa and Campbell, 1990).

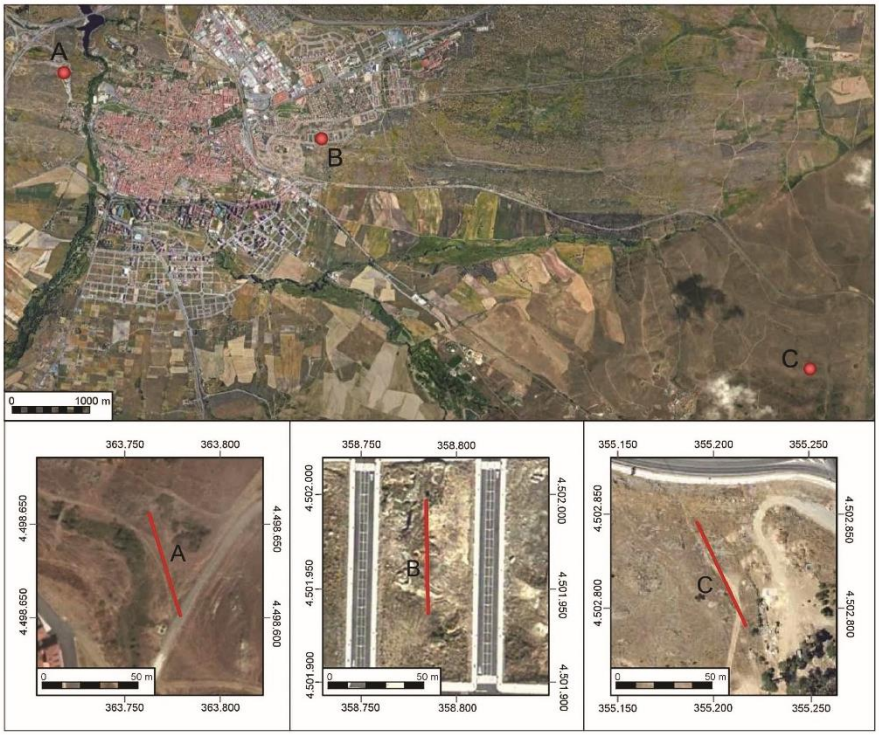

Fig. 2. Position of the seismic profiles (Geodetic Datum: WGS84, Cartographic projection: UTM, Time zone: 30). A) area 1, B) area 2, C) area 3.

Sensor RK-1 (3.9 mm in diameter and 6 cm in length) was used in the present research to measure the thermal conductivity of each sample collected from the ground. This sensor is capable of measuring the thermal conductivity in a range between 0.1 and 6 W/mK with ± 10% of accuracy and three digits of precision. Before use, it was previously calibrated with samples supplied by the manufacturer.

The relatively long read times of sensor RK-1 (around 10 min) contribute to prevent errors derived from the large diameter needle and the contact resistance between the sensor and the granular sample and solid materials. The contact between needle and tested material is guaranteed by placing thermal grease in the hole where the needle is situated. Drilling could increase the uncertainty on results. Three measurements were made in each case to evaluate the possible uncertainties.

Measurements with KD2 Pro can be strongly affected by wrong practices. To obtain the most accurate data possible, ambient temperature was kept as constant as possible during the measurement. If sample temperature changes during the measurement period, it degrades the data and makes it difficult for the inverse calculation to find the correct values for the thermal properties. To minimize these sources of error, about 15 min for samples and needle to equilibrate with the ambient temperature before taking measurements and around 15 min between readings for temperatures to equilibrate.

2.3. Methodology

2.3.1. Selection of the study areas

Three areas of known geology were chosen for the analysis of the correlation between the seismic and thermal parameters. Table 1 shows the location of these three zones, placed in the province of Avila (Spain) and the predominant geology formations in each of them. Additionally, in Fig. 1, it is possible to observe in a more exhaustive way the geological information of the mentioned areas.

2.3.2. Seismic prospecting

After selecting the study areas, the following actions were carried out:

- Tracing of profiles (50 m long in area 1 and 60 m long in areas 2 and 3) for the subsequent execution of the seismic prospecting tests (MASW and seismic refraction). Fig. 2 shows the location of these profiles.
- Execution of the seismic prospecting tests. MASW and seismic refraction tests were carried out on the profiles presented in Fig. 2.

2.3.3. Thermal conductivity tests

Thermal conductivity tests were made as follows:

- Visual exploration of each area to detect the samples with the highest degree of alteration and those samples completely compact

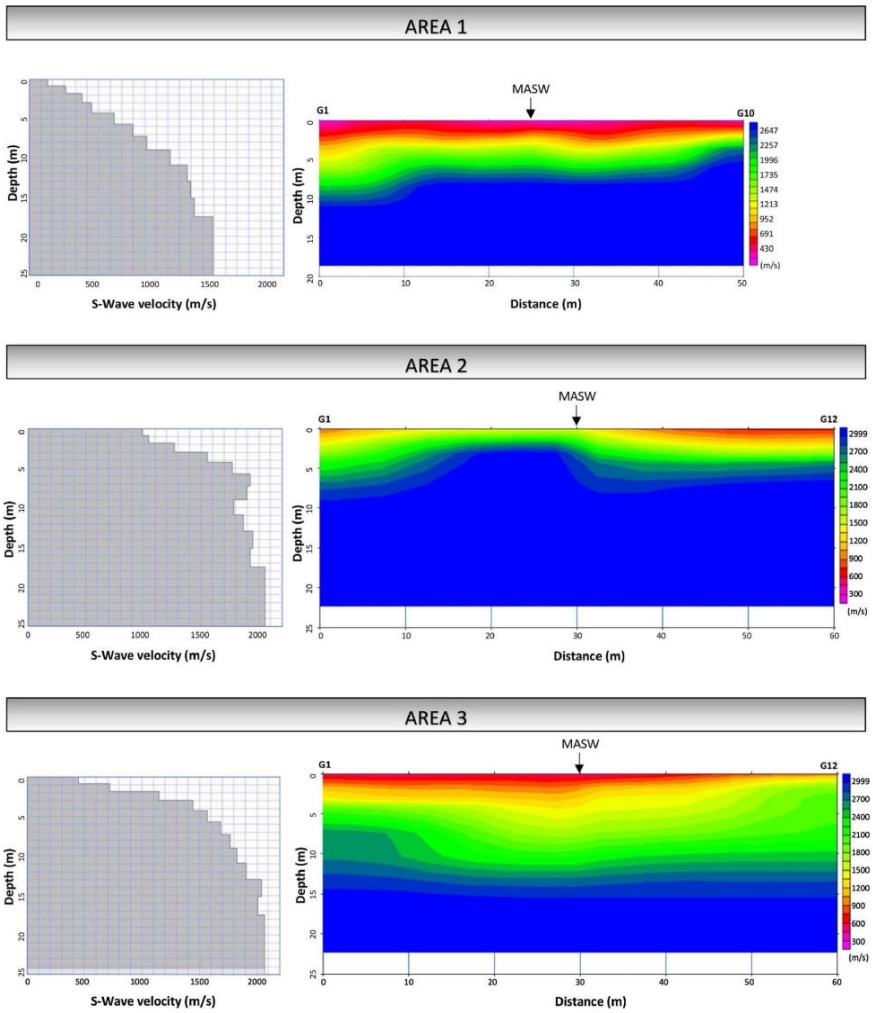

Fig. 3. Variation of the *S*-wave velocity with depth from MASW tests (on the left) and P-wave velocity distribution from seismic refraction (on the right) for each of the areas (area 1, area 2 and area 3).

and with the least degradation. Both samples belonging to the same geological formation. A set of thermal conductivity measurements were made on the most and least decomposed samples to find the lowest and highest thermal conductivity values, respectively.

- When the most and least thermal conductive samples were identified, three thermal conductivity tests were made on each of them waiting about 15 min between readings for temperatures to equilibrate.
- A specific methodology was established to carry out these tests. Loose material samples where measured in situ to reproduce its original conditions. Thirty measurements were carried out in the upper ground layer to find the most decomposed samples. Appreciable differences in the thermal conductivity parameter would be obtained in deeper layers. However, it does not constitute an inconvenient since in this research only the lowest values are required, and these values are placed in the least compact layer (the upper one). The water-saturation would also be different in deeper layers, this fact would not either affect the present work due to the reasons previously explained. Regarding compact rocky samples were taken to the laboratory to facilitate the drilling of the hole where the needle of RK-1 sensor is placed. Thirty rocky samples were collected and from these ones, the four with the highest

Table 2
Thermal conductivity results corresponding to rocks with maximum state of compaction *Standard deviation.

Area	Geological Formation	Thermal Conductivity (W/mK)					
1	***Schists***	V_1	V_2	V_3	***Mean***	σ^*	***Maximum Value***
	Sample 1	3.02	3.03	3.04	3.03	0.010	*3.12*
	Sample 2	3.13	3.12	3.12	3.12	0.007	
	Sample 3	3.01	3.03	3.01	3.01	0.014	
	Sample 4	3.11	3.11	3.11	3.11	0.000	
2	***Medium grain adamellite***	V_1	V_2	V_3	***Mean***	σ^*	***Maximum Value***
	Sample 1	2.69	2.57	2.64	2.63	0.060	*2.98*
	Sample 2	2.98	2.98	2.97	2.98	0.007	
	Sample 3	2.95	3.10	2.83	2.96	0.135	
	Sample 4	2.81	2.80	2.81	2.81	0.007	
3	***Coarse-grained adamellite***	V_1	V_2	V_3	***Mean***	σ^*	***Maximum Value***
	Sample 1	2.56	2.55	2.56	2.56	0.007	*2.56*
	Sample 2	2.36	2.36	2.41	2.38	0.002	
	Sample 3	2.47	2.45	2.48	2.47	0.016	
	Sample 4	2.45	2.45	2.46	2.45	0.007	

Table 3
Thermal conductivity results corresponding to materials with maximum state of deterioration. *Standard deviation.

Area	Geological Formation	Thermal Conductivity (W/mK)					
1	***Schists***	V_1	V_2	V_3	***Mean***	σ^*	***Maximum Value***
	Sample 1	1.57	1.57	1.56	1.57	0.007	*1.31*
	Sample 2	1.43	1.43	1.43	1.43	0.000	
	Sample 3	1.37	1.37	1.37	1.37	0.000	
	Sample 4	1.31	1.31	1.32	1.31	0.007	
2	***Medium grain adamellite***	V_1	V_2	V_3	***Mean***	σ^*	***Maximum Value***
	Sample 1	1.40	1.40	1.40	1.40	0.000	*1.04*
	Sample 2	1.11	1.11	1.11	1.11	0.000	
	Sample 3	1.00	1.10	1.01	1.04	0.055	
	Sample 4	1.31	1.31	1.31	1.31	0.000	
3	***Coarse-grained adamellite***	V_1	V_2	V_3	***Mean***	σ^*	***Maximum Value***
	Sample 1	1.01	1.02	1.02	1.01	0.010	*0.97*
	Sample 2	0.98	0.97	0.97	0.97	0.007	
	Sample 3	0.99	0.99	0.98	0.99	0.007	
	Sample 4	1.00	1.01	1.00	1.00	0.007	

Table 4
Thermal conductivity values for each *P* and *S* wave's velocities for area 1.

Depth (m)	*S*-wave velocity (m/s)	*P*-wave velocity (m/s)	Thermal Conductivity (W/mK)
0.0	157.6	379.0	1.31
0.8	314.0	523.0	1.46
1.8	454.5	798.0	1.61
3.0	536.9	991.0	1.77
4.2	732.9	1441.0	1.92
5.7	895.6	2648.0	2.07
7.3	1017.5	2711.0	2.22
9.0	1218.9	2759.0	2.37
10.9	1367.6	2808.0	2.52
13.0	1397.3	2841.0	2.67
15.1	1428.4	2857.0	2.82
17.5	1589.2	3054.0	2.97
25.0	1877.5	3090.0	3.12

thermal conductivity values were selected for the study. Rocky samples were water-saturated verifying they were totally impermeable.

Table 5
Thermal conductivity values for each *P* and *S* wave's velocities for area 2.

Depth (m)	*S*-wave velocity (m/s)	*P*-wave velocity (m/s)	Thermal Conductivity (W/mK)
0.0	989.3	1465.0	1.04
0.8	1046.1	1850.0	1.20
1.8	1269.2	2141.0	1.36
3.0	1554.2	2680.0	1.52
4.2	1770.1	3254.8	1.68
5.7	1925.6	3427.5	1.84
7.3	1894.9	3393.3	2.01
9.0	1784.8	3271.1	2.17
10.9	1866.2	3361.5	2.33
13.0	1947.0	3451.2	2.49
15.1	1925.5	3427.3	2.65
17.5	2055.2	3571.3	2.81
25.0	2216.7	3834.9	2.98

Table 6
Thermal conductivity values for each *P* and *S* wave's velocities for area 3.

Depth (m)	*S*-wave velocity (m/s)	*P*-wave velocity (m/s)	Thermal Conductivity (W/mK)
0.0	445.8	819.0	0.97
0.8	717.0	1543.0	1.11
1.8	1144.1	1685.0	1.24
3.0	1443.6	1704.0	1.37
4.2	1566.4	1802.0	1.50
5.7	1685.0	2323.0	1.63
7.3	1768.6	2468.0	1.77
9.0	1827.7	2541.0	1.90
10.9	1905.7	2654.0	2.03
13.0	2040.9	2813.0	2.16
15.1	2007.4	3120.0	2.29
17.5	2069.2	3345.0	2.43
25.0	2075.0	3548.6	2.56

2.3.4. Relation between seismic prospecting and thermal conductivity measurements

An analysis of the seismic and thermal conductivity results was made to establish a correlation between the propagation velocity of the *P* and *S* waves and the thermal conductivity of samples from the same material.

From the connection of the lowest and highest thermal conductivity values with *P* and *S* wave's velocities, a correlation pattern was created for each of the areas.

In this way, this method is really useful whenever a geothermal installation is placed on geology formations similar to the ones of the study. Seismic prospecting will allow knowing the ground composition and at the same time the thermal conductivity of the surrounding ground.

3. Results

3.1. Seismic parameters

Seismic prospecting allowed knowing the *S* and *P* waves velocity as a function of depth in each area. On the one hand, MASW tests results provided the *S* wave velocity from surface to a depth of 25 m. On the other hand, *P* waves velocity was obtained from the seismic refraction tests carried out on the profiles shown in Fig. 2.

3.1.1. MASW

MASW results are shown in Fig. 3. This figure graphically shows how *S*-wave velocity changes with depth. From *S*-wave velocities and depths, a series of parameters were also calculated for each of the study areas. Tables A1–A3 presented in the Appendix A show these parameters obtained from secondary calculations that are very useful to

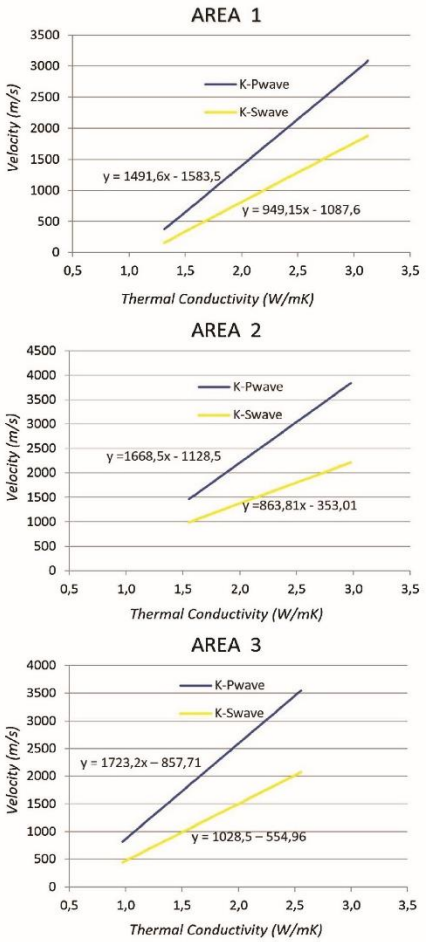

Fig. 4. Thermal conductivity versus *P* and *S* wave's velocities for each area. A) Area 1, B) Area 2, C) Area 3.

characterise each geological formation.

S-wave velocity values presented in Tables A1–A3 were used in the corresponding correlation with the thermal conductivity measurements presented in *Section* 3.2. *Thermal conductivity results.*

3.1.2. Seismic refraction

Seismic refraction prospecting provided the evolution of P-waves velocity from surface to a depth of 20 m and along 50 m for area 1 (length of profile 1) and 60 m for the rest of areas 2 and 3. These results (also presented in Fig. 3), are shown as sections with different tonalities depending on the P-wave velocity.

Graphs shown on the right side of Fig. 3 allow obtaining the *P*-wave velocity values for any point in depth and length. Values corresponding to MASW position (in different depths) have been correlated with the thermal conductivity measurements.

3.2. Thermal conductivity results

Thermal conductivity results are shown in Tables 2 and 3. Table 2 presents the maximum thermal conductivity values corresponding to the state of lowest degradation of each formation. On the contrary, Table 3 collects the minimum thermal conductivity values corresponding to the state of highest degradation. The methodology consisted of the realization of several thermal conductivity tests on different samples. As already mentioned, thirty measurements were carried out in the field on the most decomposed materials as well as thirty rocky specimens were measured in the laboratory. This work methodology allowed identifying the most and least decomposed materials of each area, selecting the final samples to be considered in the present research. From each of these samples (Samples 1, 2, 3 and 4) three measurements were made to verify the results (V_1, V_2 and V_3). For each case, the lowest and highest values are shown in Tables 2 and 3, the mean of them, and finally the maximum/minimum value.

Maximum and minimum thermal conductivity values presented in Tables 2 and 3 were subsequently related with *P* and *S* wave's velocities as shown in the next section.

3.3. Correlation of S and P waves velocities with thermal conductivities

The correlation between the *P* and *S* wave's velocities and the values of thermal conductivities are shown below for each of the study areas. *P*-waves velocities were taken from the seismic refraction results and calculated in the position of the MASW test in each profile. *S*-waves velocities were directly taken from MASW tests.

The minimum thermal conductivity values (of the whole area) presented in Table 3 have associated the lowest *P* and *S* waves' velocity of the same global area. On the contrary, the maximum thermal conductivity values from Table 2 are associated to the highest *P* and *S* waves' velocity. Specific combinations of thermal conductivities and velocities data corresponding to the same point were not carried out. A straight line connects both correlations, so the equation of this line is used to calculate the intermediate values. The following sections show numerically and graphically the connection among the mentioned parameters for each area.

The correlations between *P* and *S* wave's velocities and the thermal conductivities values are shown in Table 4 (area 1), Table 5 (area 2) and Table 6 (area 3). Fig. 4 graphically presents the mentioned correlations for the three study areas. The lowest and highest thermal conductivity values measured in each of the areas were associated to the lowest and highest P and S wave velocities. Based on these initial and final points, the rest of wave's velocities values from the seismic prospecting were given a thermal conductivity value following the equation obtained in each case (Fig. 4).

4. Discussion

4.1. Data collection and processing

The most laborious task when carrying out this work was the data collection to measure the maximum and minimum thermal conductivity values. The study of any formation requires the collection of sufficient representative samples. In this case, the thermal conductivity of samples from continuous profiles was measured in situ (loose

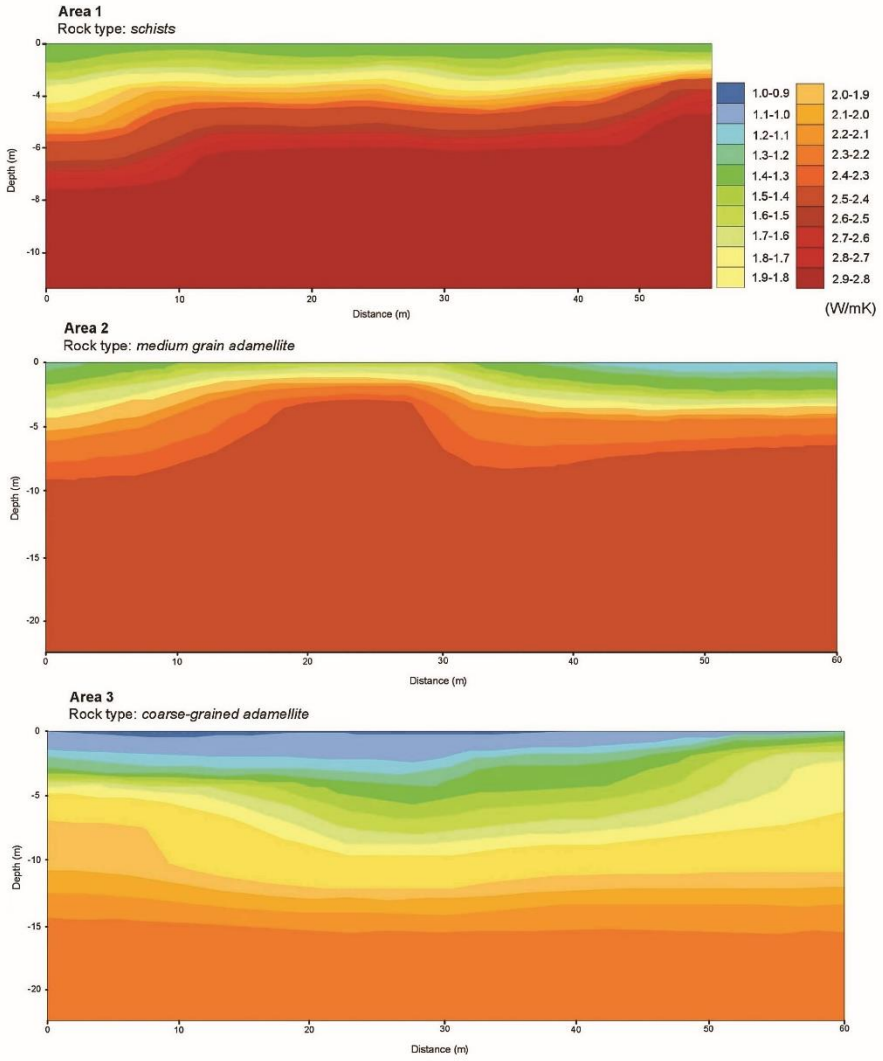

Fig. 5. 2D thermal conductivity image of the ground. A) area 1, B) area 2 and C) area 3.

material) or in the laboratory (rocky samples). An arduous methodology was followed to detect the most/least decomposed material, that is to say, the samples with the highest/lowest thermal conductivity in each area. Once detected the mentioned samples, the thermal conductivity measuring was properly verified due to the large number of measurements made in each case. Additionally, the validity of these measurements was confirmed by comparing the results with the ones commonly accepted at the *"Technical Code of Building"* (CTE) for each geological formation (Constructive Solutions Compendium, 2007).

Relating the seismic prospecting, there were not significant

difficulties in the process of field measuring. P and S wave's velocities are representative of an area in question and it is difficult to compare those values with the ones of similar formations. This fact is due to the different conditions (pressure, compaction, humidity…) experienced in each case.

4.2. Method

Seismic velocities known from MASW and seismic refraction measurements have been used as secondary variables for estimating the thermal conductivity of the surrounding ground at a very low enthalpy borehole heat exchanger. *P* and *S* waves velocities are typically easier to obtain and more readily than sparse thermal conductivity values. Considering the similar trends between seismic waves and heat conduction, thermal conductivity values can be estimated from an interpolation of seismic profiles. It is important to highlight that seismic velocity qualitatively encompasses information of the ground, such as rock fracturing or possible heterogeneities in the rock lithology that can be identified from the different seismic velocities they cause. This information can be also used to interpolate the thermal conductivities of rocks in space. The quality of this interpolation will depend mainly on the closeness of the general trend between both variables. As shown in Fig. 4, from *P* or *S* wave's velocities, the corresponding thermal conductivity value can be known in each of the study areas.

The presented research shows valid and reasonable results for three different geological formations. These results can be used for future measurements of geothermal installations placed in these lithologies. For this reason, the method is limited to similar areas to the ones considered in this study. Studies about other formations will be performed in future.

The correlation *P* wave velocity-thermal conductivity is supported by a large number of researches (Zamora et al., 1993; Boulanouar et al., 2012; Gu et al., 2017). In this study, MASW prospecting provided *S* wave velocities which allowed having an additional source of correlation. It is also important to highlight the lack of previous works focused on the same rock types. Thus, the present research constitutes a useful tool when dimensioning a geothermal installation in similar geological formations.

Appendix A

Additional information is presented in Tables A1–A3, and .

5. Conclusions

Thanks to the development of these types of methodologies, it is possible to predict the thermal behaviour of geological formations. From MASW and seismic refraction tests together with thermal conductivity measurements, graphs of thermal conductivity against P and S wave's velocities have been presented (Fig. 4). From these graphs a 2D thermal conductivity image of the subsoil was obtained for each study area. These images, shown in Fig. 5, allow knowing the thermal conductivity of the different layers of the ground.

Knowing the real thermal conductivity of a certain geological formation is really useful when making the preliminary measuring of a very low enthalpy geothermal system. An appropriate estimation of the thermal conductivity parameter of the surrounding ground can avoid important over-measurements with the consequent economic saving. A slight variation of this parameter has a huge influence in the total drilling length of the borehole.

From a general perspective the results confirm that geophysical methods (MASW and seismic refraction) are of great value to evaluate the thermal conductivities of rocks in geothermal reservoirs. Apart from the general geological information provided by these methods, they also constitute a helpful practice in geothermal reservoir modelling in the depth of the present research.

Future researches in areas of different geology will complete the present work making it available to be used in a wider range of geothermal systems.

Acknowledgments

Authors would like to thank the Department of Cartographic and Land Engineering of the Higher Polytechnic School of Avila, University of Salamanca, for allowing us to use their facilities and their collaboration during the experimental phase of this research. Authors also want to thank the Ministry of Education, Culture and Sport for providing a FPU Grant (Training of University Teachers Grant) to the corresponding author of this paper what has made possible the realization of the present work.

Table A1
Parameters obtained from MASW tests in area 1.

Depth (m)	*S*-wave velocity (m/s)	Density (g/cm^3)	N − SPT (n° of hits)	Poisson coefficient "μ"	Young's modulus "*E*" (GPa)	Cutting modulus "*G*" (GPa)	Compressibility modulus "*K*" (GPa)
0.0	157.6	1.777	4.695	0.395	0.123	0.044	0.196
0.8	314.0	1.832	42.120	0.218	0.440	0.180	0.260
1.8	454.5	1.880	136.866	0.260	0.978	0.388	0.679
2.96	536.9	1.908	232.633	0.292	1.421	0.550	1.140
4.2	732.9	1.972	626.772	0.326	2.808	1.059	2.682
5.7	895.6	2.024	1186.543	0.435	4.658	1.622	12.022
7.3	1017.5	2.061	1781.919	0.418	6.050	2.133	12.299
9.0	1218.9	2.121	3166.991	0.379	8.687	3.150	11.939
10.9	1367.6	2.163	4568.773	0.345	10.877	4.045	11.660
13.0	1397.3	2.172	4892.658	0.340	11.364	4.239	11.871
15.2	1428.4	2.180	5247.748	0.333	11.859	4.447	11.862
17.5	1589.2	2.224	7371.032	0.314	14.761	5.615	13.250
25.0	1877.5	2.298	12534.741	0.207	19.558	8.099	11.139

Table A2
Parameters obtained from MASW tests in area 2.

Depth (m)	S-wave velocity (m/s)	Density (g/cm^3)	N − SPT (n° of hits)	Poisson coefficient "μ"	Young's modulus "E" (GPa)	Cutting modulus "G" (GPa)	Compressibility modulus "K" (GPa)
0.0	989.3	2.053	1629.395	0.081	4.341	2.008	1.726
0.8	1046.1	2.070	1946.402	0.265	5.729	2.264	4.062
1.8	1269.2	2.136	3602.445	0.229	8.454	3.439	5.200
3.0	1554.2	2.215	6866.726	0.247	13.334	5.348	8.771
4.2	1770.1	2.271	10390.786	0.290	18.355	7.114	14.569
5.7	1925.6	2.310	13587.210	0.269	21.742	8.564	15.712
7.3	1894.9	2.303	12908.598	0.273	21.051	8.266	15.486
9.0	1784.8	2.275	10667.931	0.288	18.664	7.245	14.676
10.9	1866.2	2.296	12296.397	0.277	20.416	7.992	15.274
13.0	1947.0	2.316	14073.677	0.267	22.228	8.775	15.870
15.2	1925.5	2.310	13582.999	0.269	21.737	8.562	15.711
17.5	2055.2	2.342	16719.029	0.252	24.766	9.887	16.671
25.0	2216.7	2.396	21273.474	0.249	29.404	11.770	19.533

Table A3
Parameters obtained from MASW tests in area 3.

Depth (m)	S-wave velocity (m/s)	Density (g/cm^3)	N − SPT (n° of hits)	Poisson coefficient "μ"	Young's modulus "E" (GPa)	Cutting modulus "G" (GPa)	Compressibility modulus "K" (GPa)
0.0	445.8	1.890	128.674	0.289	0.969	0.376	0.767
0.8	717.0	1.972	584.310	0.362	2.762	1.014	3.343
1.8	1144.1	2.091	2588.448	0.072	5.867	2.736	2.286
3.0	1443.6	2.171	5427.848	0.771	2.069	4.522	0.271
4.2	1566.4	2.199	7040.047	1.046	0.497	5.393	0.054
5.7	1685.0	2.230	8881.790	0.055	11.958	6.328	3.590
7.3	1768.6	2.255	10363.110	0.028	13.709	7.051	4.329
9.0	1827.7	2.273	11506.272	0.036	14.637	7.592	4.551
10.9	1905.7	2.294	13143.163	0.032	16.119	8.327	5.048
13.0	2040.9	2.325	16351.707	0.056	18.286	9.683	5.484
15.1	2007.4	2.314	15510.472	0.147	21.380	9.321	10.090
17.5	2069.2	2.325	17084.694	0.190	23.690	9.953	12.739
25.0	2075.0	2.325	17237.326	0.240	24.826	10.009	15.927

References

Özkahraman, H.T., Selver, R., I-sik, E.C., 2004a. Determination of the thermal conductivity of rock from P-wave velocity. Int. J. Rock Mech. Min. Sci. 41, 703–708.

Özkahraman, H.T., Selver, R., Isik, E.C., 2004b. Determination of the thermal conductivity of rock from P-wave velocity. Int. J. Rock Mech. Min. Sci. 41, 703–708.

Balling, N., Kristiansen, J.I., Breiner, N., Poulsen, K.D., Rasmusen, R., Saxov, S., 1981. Geothermal measurements and subsurface temperature modelling in Denmark. Geol. Skr. 16 (1), 172.

Barry-Macaulay, D., Bouazza, A., Singh, R.M., Wang, B., Ranjith, P.G., 2013. Thermal conductivity of soils and rocks from the Melbourne (Australia) region. Eng. Geol. 164, 131–138.

Blázquez, C.S., Martín, A.F., García, P.C., Sánchez Pérez, L.S., del Caso, S.J., 2016. Analysis of the process of design of a geothermal installation. Renew. Energ. 89 (1), 188–199.

Blázquez, Cristina Sáez, Martín, Arturo Farfán, Nieto, Ignacio Martín, García, Pedro Carrasco, Sánchez Pérez, Luis Santiago, Aguilera, Diego González, 2017. Thermal conductivity map of the Avila region (Spain) based on thermal conductivity measurements of different rock and soil samples. Geothermics 65, 60–71.

Boulanouar, A., Rahmouni, A., Boukalouch, M., Géraud, Y., El Amrani El Hassani, I., Harnafi, M., Sebbanic, M.J., 2012. A Correlation between P-wave velocity and thermal conductivity of heterogeneous porous materials. MATEC Web Conf. 2. http://dx.doi.org/10.1051/mateconf/20120205004.

Cermak, V., Rybach, L., 1982. Thermal conductivity and specific heat of minerals and rocks. In: Beblo, M. (Ed.), Geophysics − Physical Properties of Rocks, 1. Springer, pp. 305–343.

Constructive Solutions Compendium, 2007. Código Técnico de la Edificación. Instituto de Ciencias de la Construcción Eduardo Torroja e Instituto de Ciencias de la Construcción de Castilla y León, Castilla y León, Spain.

Decagon Devices, 2016. KD2 Pro Thermal Properties Analyzer Operator's Manual. Decagon Devices, Inc.

Esteban, L., Pimienta, L., Sarout, J., Piane, C.D., Haffen, S., Geraud, Y., Timms, N.E., 2015. Study cases of thermal conductivity prediction from P-wave velocity and porosity. Geothermics 53, 255–269.

Fuchs, S., Balling, N., 2016a. Improving the temperature predictions of subsurface thermal models by using high-quality input data. Part 1: Uncertainty analysis of the thermal-conductivity parameterization. Geothermics 64, 42–54.

Fuchs, S., Balling, N., 2016b. Improving the temperature predictions of subsurface thermal models by using high-quality input data. Part 2: A case study from the Danish-German border region. Geothermics 64, 1–14.

Fuchs, S., Förster, A., 2014. Well-log based prediction of thermal conductivity of sedimentary successions: examples from the North German Basin. Geophys. J. Int. 196, 291–311.

Fuchs, S., Balling, N., Förster, A., 2015. Calculation of thermal conductivity, thermal diffusivity and specific heat capacity of sedimentary rocks using petro physical well logs. Geophys. J. Int. 203 (3), 1977–2000.

Gegenhuber, N., Schoen, J., 2012. New approaches for the relationship between compressional wave velocity and thermal conductivity. J. Appl. Geophys. 76, 50–55.

Gegenhuber, N., 2011. Compressional wave velocity-thermal conductivity correlation – From the laboratory to logs. Society of Petroleum Engineers – 73rd European Association of Geoscientists and Engineers Conference and Exhibition 2011 – Incorporating SPE EUROPEC.

Gu, Yixi, Rühaak, Wolfram, Bär, Kristian, Sass, Ingo, 2017. Using seismic data to estimate the spatial distribution of rock thermal conductivity at reservoir scale. Geothermics 66, 61–72.

Haenel, R., Rybach, L., Stegena, L., 1988. Thermal exploration methods. In: Haenel, R., Stegena, L., Rybach, L. (Eds.), Handbook of Terrestrial Heat-Flow Density Determination, Chapter 2. Kluwer Academic Publishers, Dordrecht.

Hartmann, A., Pechnig, R., Clauser, C., 2008. Petro physical analysis of regional scale thermal properties for improved simulations of geothermal installations and basin scale heat and fluid flow. Int. J. Earth Sci. 97 (2), 421–433.

Jorand, R., Vogt, C., Marquart, G., Clauser, C., 2013. Effective thermal conductivity of heterogeneous rocks from laboratory experiments and numerical modeling. J. Geophys. Res.: Solid Earth 118, 5225–5235.

Kluitenberg, G.J., Ham, J.M., Bristow, K.L., 1993. Error analysis of the heat pulse method for measuring soil volumetric heat capacity. Soil Sci. Soc. Am. J. 57, 1444–1451.

Krishnaiah, S., Singh, D.N., Jadhav, G.N., 2004. A methodology for determining thermal properties of rocks. Min. Sci. 1 (5), 877–882.

Kukkonen, Lindberg, 1995. Thermal Conductivity of Rocks at the TVO Investigation Sites Olkiluoto, Romuvaara and Kivetty. Nuclear Waste Commission of Finnish Power Companies, Report YJT-95-08. pp. 29.

Liou, Jyh-Chau, Tien, Neng-Chuan, 2016. Estimation of the thermal conductivity of granite using a combination of experiments and numerical simulation. Int. J. Rock Mech. Min. Sci. 81, 39–46.

Lira-Cortés, L., GonzálezRodríguez, O.J., Méndez-Lango, E., 2008. Sistema de Medición de la Conductividad Térmica de Materiales Sólidos Conductores, Diseño y Construcción. In: Simposio de Metrología Santiago de Querétaro. México.

Louie, John N., 2001. Shear-Wave velocity to 100 meters depth from refraction

microtremor arrays. Bull. Seismol. Soc. Am. 91, 347–364.
Park, Choon B., Miller, Richard D., Xia, Jianghai, 1999. Multichannel analysis of surface waves. Geophysics 64 (3), 800–808.
Pimienta, L., Sarout, J., Esteban, L., Piane, C.D., 2014. Prediction of rocks thermal conductivity from elastic wave velocities, mineralogy and microstructure. Geophys. J. Int. 197 (2).
Popov, Y., Tertychnyi, Y., Romushkevich, R., Korobkov, D., Pohl, J., 2003. Interrelations between thermal conductivity and other physical properties of rocks: experimental data. Pure Appl. Geophys. 160, 1137–1161.
Popov, Yu., Beardsmore, G., Clauser, C., Roy, S., 2016. ISRM suggested methods for determining thermal properties of rocks from laboratory tests at atmospheric pressure. Rock Mech. Rock Eng. 49 (10), 4179–4207.
Rühaak, W., Guadagnini, A., Geiger, S., Bär, K., Gu, Y., Aretz, A., Homuth, S., Sass, I., 2015. Upscaling thermal conductivities of sedimentary formations for geothermal exploration. Geothermics 58, 49–61.
Rühaak, W., 2015. 3-D interpolation of subsurface temperature data with known measurement error using Kriging. Environ. Earth Sci. 73 (4), 1893–1900.
Shiozawa, S., Campbell, G.S., 1990. Soil thermal conductivity. Remote Sens. Rev. 5, 301–310.
Zamora, Maria, Vo-Thanh, Dung, Bienfait, Gérard, Poirier, Jean Paul, 1993. An empirical relationship between thermal conductivity and elastic wave velocities in sandstone. Geophys. Res. Lett. 20, 1679–1682.